

PAPER • OPEN ACCESS

On the bending vibration of a train driving wheelset

To cite this article: T Mazilu and M A Gheti 2019 *IOP Conf. Ser.: Mater. Sci. Eng.* **591** 012059

View the [article online](#) for updates and enhancements.

On the bending vibration of a train driving wheelset

T Mazilu and M A Gheti

Politehnica University of Bucharest, Department of Railway Vehicles,
313 Splaiul Independentei, 060042, Bucharest, Romania

E-mail: trmazilu@yahoo.com

Abstract. The driving wheelset is used on the traction railway vehicle to support a part of the vehicle's weight and for traction and braking purpose. The driving wheelset consists of the axle on which the two wheels and the driving gear are rigidly attached. The bending vibrations in the driving wheelset may be caused by variations of the vertical wheel/rail contact force. In this paper, a mechanical model of the driving wheelset, consisting of a free-free uniform beam with three rigid bodies, representing the axle, the two wheels and the driving gear, is considered. Using an analytical method for solving the equations of motion for the model, the steady-state harmonic behaviour of the bending vibrations is analysed. The frequency response function and the impact of the position of the driving gear upon this function are pointed out.

1. Introduction

The wheelset is one of the most important machine parts of a rail vehicle, helping to drive the vehicle along the track, guiding it and transferring the load forces from the vehicle to the track.

The wheelset-track vibrations are structural vibrations. However, at low frequencies, the wheels and the axle vibrate together as a rigid body for both vertical and lateral wheelset-track vibrations. In the domain of medium frequencies, the wheelset vibration is influenced by the axle bending vibrations. At high frequencies, above 1500 Hz for radial vibration and 4-500 Hz for axial ones, the wheel tread is decoupled by the hub and these modes influences the wheelset vibration [1].

Wheelsetsexhibit a broad-spectrum vibration, which is interesting from many technical viewpoints: rolling noise [2], wear of the wheel-railcontacts surfaces [3], traction performance [4].

The following models may be used to study the wheelset vibrations: rigid body models in which the wheelset is taken as a simply rigid body [5] or is divided into several rigid parts coupled by elastic and damping elements [6]; structural models composed of continuous elastic bodies, with which it can obtain a correct representation of wheelset inertia and elasticity distribution [7], and models based on the finite element method, allowing for high accuracy in calculating the eigenmodes, especially at high frequencies [8, 9].

In this paper a model with distributed and concentrated parameters is developed to study the bending vibrations of a driving wheelset in the low and medium frequencies range up to 200-300Hz. Using the modal analysis method, the basic characteristics of the driving wheelset vibration are emphasized.

2. Mechanical model

Generally, the axle of the wheelset can be modelled as aEuler-Bernoulli beam or as a Timoshenko beam. The advantage of the Euler-Bernoulli beam is the simplicity, while using the Timoshenko beam model offers better precision of calculations due to consideration of the effect of the shear force on the



rotation of the beam cross-sections as well as the inertial effect of those rotations. The Euler-Bernoulli beam model can be applied with good results in situations where the bending wavelength is greater than the circumference of the wheelset cross section.

The mechanical model for studying the bending vibrations of the wheelset (figure 1) consists of a uniform free-free Euler-Bernoulli beam, which has attached lumped masses representing the two wheels and the gear.

The following assumptions are adopted: the cross sections of the beam are plane and normal to the neutral axis, the effect of the shear force and the inertial effect of the rotation of the cross-sections are neglected, the gyroscopic effect due to the rotation of the driven wheelset is not taken into consideration.

The beam has the mass per unit length equal to $m = \rho S$ where ρ is the density of the material and S represents the cross-section area, and the bending stiffness EI in which E is Young's modulus and I is the moment of inertia of the cross-section. The wheels have the lumped mass M_r and the moment of inertia J_r , and the wheelset gear has the lumped mass M_c and the moment of inertia J_c . The wheels are located at distance a from the wheelset ends and the gear is located at distance c . The distance between the wheel's nominal running circles is $2e$.

Wheelset movement is related to a fixed reference system Oxz .

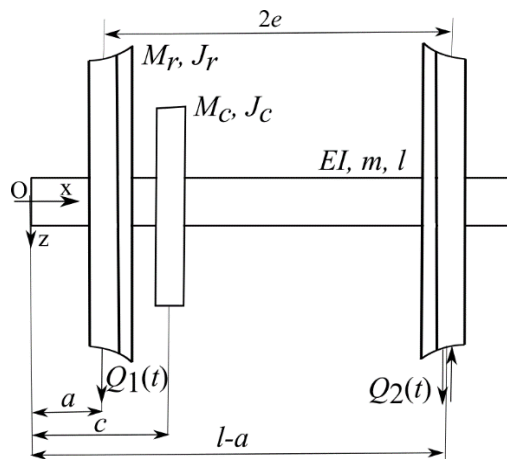


Figure 1. The mechanical model of a driving wheelset.

The vertical forces $Q_1(t)$ and $Q_2(t)$ depending on the time t act on the two wheels. These forces act in the same or opposite directions. The justification for this assumption is related to the fact that any excitation Q_1, Q_2 can be decomposed into a symmetrical excitation and an antisymmetric excitation

$$\begin{bmatrix} Q_1 \\ Q_2 \end{bmatrix} = \begin{bmatrix} Q_1^+ \\ Q_1^+ \end{bmatrix} + \begin{bmatrix} Q_2^- \\ -Q_2^- \end{bmatrix} \quad (1)$$

where $Q_1^+ = (Q_1 + Q_2)/2$ is the magnitude of the symmetrical excitation and $Q_2^- = (Q_1 - Q_2)/2$ is the magnitude of the antisymmetric excitation.

The equation (2) of motion for the driving wheelset is:

$$\begin{aligned} & EI \frac{\partial^4 w(x,t)}{\partial x^4} + m \frac{\partial^2 w(x,t)}{\partial t^2} + M_r \left[\frac{\partial^2 w(a,t)}{\partial t^2} \delta(x-a) + \frac{\partial^2 w(l-a,t)}{\partial t^2} \delta(x-l+a) \right] - \\ & - J_r \left[\frac{\partial^3 w(a,t)}{\partial x \partial t^2} \delta'(x-a) + \frac{\partial^3 w(l-a,t)}{\partial x \partial t^2} \delta'(x-l+a) \right] + M_c \frac{\partial^2 w(c,t)}{\partial t^2} \delta(x-c) - J_c \frac{\partial^3 w(c,t)}{\partial x \partial t^2} \delta'(x-c) = \\ & = Q_1(t) \delta(x-a) + Q_2(t) \delta(x-l+a). \end{aligned} \quad (2)$$

where $\delta(\cdot)$ is the Dirac function and x represents the space coordinate along the axle.

Applying the modal analysis method, the vertical displacement of the wheelset transverse sections shall be considered as equation (3):

$$w(x,t) = w_0(t) + \left(x - \frac{l}{2}\right)\theta_0(t) + \sum_{n=2}^{\infty} X_n(x)T_n(t) \tag{3}$$

where $w_0(t)$ represents the time coordinate for the first rigid vibration mode (vertical translation), $\theta_0(t)$ represents the time coordinate of the second rigid vibration mode (vertical rotation with respect to the centre of the beam) with its eigen function $x-l/2$, and $X_n(x)T_n(t)$ are the elastic vibration modes with the time coordinate $T_n(t)$ and the eigen function given by equation (4):

$$X_n(x) = \sin\beta_n x + \sinh\beta_n x - \frac{\sin\beta_n l - \sinh\beta_n l}{\cos\beta_n l - \cosh\beta_n l} (\cos\beta_n x + \cosh\beta_n x) \tag{4}$$

where β_n results from characteristic equation.

The frequency response of the driving wheelset is based on the modal analysis method applied to equation (2), in which the two rigid vibration modes and the first two elastic vibration modes are considered.

The equations of motion for a vibration mode is obtained by multiplying the equation (2) by its eigen function, followed by integration in the $[0, l]$ domain. Applying the orthogonality property of the eigen modes, the following equations of motion are obtained, equations (5) - (8):

$$(ml + 2M_r + M_c)\ddot{w}_0(t) + pM_c\ddot{\theta}_0(t) + (2M_r X_2(a) + M_c X_2(c))\ddot{T}_2(t) + M_c X_3(c)\ddot{T}_3(t) = Q_1(t) + Q_2(t) \tag{5}$$

$$pM_c\ddot{w}_0(t) + \left(m\frac{l^3}{12} + 2M_r e^2 + p^2 M_c + 2J_r + J_c\right)\ddot{\theta}_0(t) + pM_c X_2(c)\ddot{T}_2(t) + J_c X_2'(c)\ddot{T}_2(t) - 2eM_r X_3(a)\ddot{T}_3(t) + 2J_r X_3'(a)\ddot{T}_3(t) + pM_c X_3(c)\ddot{T}_3(t) + J_c X_3'(c)\ddot{T}_3(t) = e(Q_2(t) - Q_1(t)) \tag{6}$$

$$(2M_r X_2(a) + M_c X_2(c))\ddot{w}_0(t) + (-eM_c X_2(c) + J_c X_2'(c))\ddot{\theta}_0(t) + k_2 \cdot T_2 + (M_2 + 2M_r X_2(a)^2 + M_c X_2(c)^2 + 2J_r X_2'(a)^2 + J_c X_2'(c)^2)\ddot{T}_2(t) + (M_c (X_2(c) X_3(c)) + J_c (X_2'(c) X_3'(c)))\ddot{T}_3(t) = X_2(a)(Q_1(t) + Q_2(t)) \tag{7}$$

$$(M_c X_3(c))\ddot{w}_0(t) + (-2eM_r X_3(a) + pM_c X_3(c) + 2J_r X_2'(a) + J_c X_2'(c))\ddot{\theta}_0(t) + k_3 T_3(t) + M_3 \ddot{T}_3(t) + (M_c (X_3(c) X_2(c)) + J_c (X_2'(c) X_3'(c)))\ddot{T}_2(t) + (2M_r X_3(a)^2 + M_c X_3(c)^2 + 2J_r X_3'(a)^2 + J_c X_3'(c)^2)\ddot{T}_3(t) = X_3(a)(Q_1(t) - Q_2(t)), \tag{8}$$

where $e = (l/2 - a)$, $p = (c - l/2)$, $m_{2,3}$ are the modal masses, $k_{2,3}$ are the modal stiffness, with

$$k_{2,3} = EI \int_0^l (X_{2,3}''(x))^2 dx \text{ and } M_{2,3} = m \int_0^l (X_{2,3}(x))^2 dx .$$

Considering the steady state harmonic behaviour, the time functions and the external forces have the bellow forms, equation (9):

$$w_0(t) = W_0 \sin(\omega t); \theta_0(t) = \Theta_0 \sin(\omega t); T_{2,3}(t) = T_{2,3} \sin(\omega t); Q_{2,3}(t) = Q_{2,3} \sin(\omega t), \quad (9)$$

where W_0 , Θ_0 , $T_{2,3}$ and $Q_{1,2}$ are the amplitudes, and ω is the angular frequency.

The frequency response is determined by solving a system formed with the following equations, (equations (10) – (13)):

$$\begin{aligned} & -\omega^2 (ml + 2M_r + M_c)W_0 - \omega^2 pM_c \Theta_0 - \\ & -\omega^2 (2M_r X_2(a) + M_c X_2(c))T_2 - \omega^2 M_c X_3(c)T_3 = Q_1 + Q_2 \end{aligned} \quad (10)$$

$$\begin{aligned} & -\omega^2 pM_c W_0 - \omega^2 \left(m \frac{l^3}{12} + 2M_r e^2 + p^2 M_c + 2J_r + J_c \right) \Theta_0 - \omega^2 (pM_c X_2(c) + J_c X_2'(c))T_2 + \\ & -\omega^2 (-2eM_r X_3(a) + 2J_r X_3'(a) - eM_c X_3(c) + J_c X_3'(c))T_3 = e(Q_2 - Q_1) \end{aligned} \quad (11)$$

$$\begin{aligned} & -\omega^2 (2M_r X_2(a) + M_c X_2(c))W_0 - \omega^2 (-eM_c X_2(c) + J_c X_2'(c))\Theta_0 + \\ & + k_2 \cdot T_2 - \omega^2 (M_2 + 2M_r X_2(a)^2 + M_c X_2(c)^2 + 2J_r X_2'(a)^2 + J_c X_2'(c)^2)T_2 - \\ & -\omega^2 (M_c (X_2(c)X_3(c)) + J_c (X_2'(c)X_3'(c)))T_3 = X_2(a)(Q_1 + Q_2) \end{aligned} \quad (12)$$

$$\begin{aligned} & -\omega^2 (M_c X_3(c))W_0 - \omega^2 (-2eM_r X_3(a) + pM_c X_3(c) + 2J_r X_3'(a) + J_c X_3'(c))\Theta_0 + \\ & + k_3 T_3 - \omega^2 M_3 T_3 - \omega^2 (M_c (X_3(c)X_2(c)) + J_c (X_3'(c)X_2'(c)))T_2 + \\ & -\omega^2 (2M_r X_3(a)^2 + M_c X_3(c)^2 + 2J_r X_3'(a)^2 + J_c X_3'(c)^2)T_3 = X_2(a)(Q_1 - Q_2). \end{aligned} \quad (13)$$

For symmetric excitation, the amplitudes of the external forces are $Q_1=Q_2=Q$, and for antisymmetric excitation, the external forces amplitudes will be $Q_1=-Q_2=Q$.

3. Numerical application

In this section, the model and method above presented are used to analyse the harmonic steady-state behaviour of a wheelset. The parameters for the model are as follows: axle length $l = 2.11$ m, axle diameter $d = 0.1991$ m, Young's modulus $E = 210$ GPa, the density of the material is $\rho = 7850$ kg/m³, the wheel mass is $M_r = 500$ kg, the moment of inertia of the wheel is $J_r = 48.82$ kgm², the mass of the crown is $M_c = 350$ kg, the moment of inertia of the toothed crown is $J_c = 17$ kgm², the distance between the axle and wheel end is $a = 0.305$ m and the distance between the axle end and the toothed crown is $c = 0.52$ m. The parameters values correspond to a driving wheelset equipping the 060EA electric locomotive of the Romanian Railway. The frequency range considered is between 10 and 300 Hz.

At first, the case of the wheelset without gear is analysed as a geometric and inertial symmetrical structure. Figure 2 shows the calculated receptance at the first wheel of rigid vibration mode and the first elastic vibration mode when the wheelset is symmetrically excited. It can be seen that on the frequency range considered, the rigid vibration mode is predominant. The resonance frequency is 95.5 Hz. The receptance of the elastic vibration mode is similar to a system with a single degree. The two symmetrical vibration modes are shown in figure 3. The resonance frequency is preceded by an antiresonance frequency at 94 Hz. In this case, the receptances are equal for the two wheels.

If the wheelset is antisymmetric excited, then its response is made up by the rigid antisymmetric (rotation) mode and the first antisymmetric elastic mode. The receptances of these two vibration modes calculated at the first wheel are shown in figure 4 and the total receptance in figure 5. The

second rigid vibration mode is predominant over the elastic mode of antisymmetric vibration over the entire range of frequencies considered. The antisymmetric wheelset vibration receptance has an antiresonance with frequency of 192.5 Hz, followed by a resonance at approximately 205 Hz. The receptances are equal and opposite for the two wheels. This is similar to a mechanical system equivalent to two degrees of freedom, elastically coupled, one of which has rigid movement.

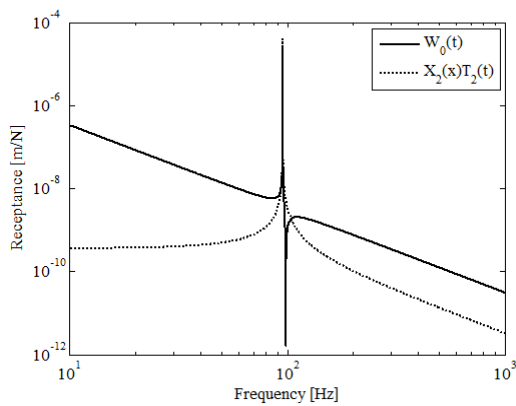


Figure 2. Symmetric eigenmodes.

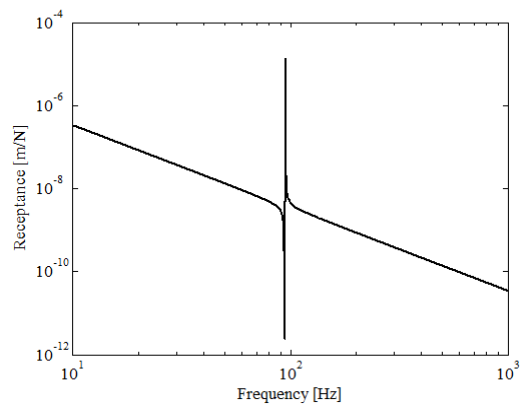


Figure 3. Wheelset receptance for symmetric excitation.

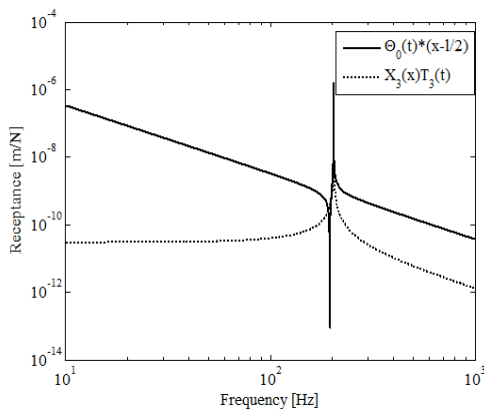


Figure 4. Antisymmetric eigenmodes.

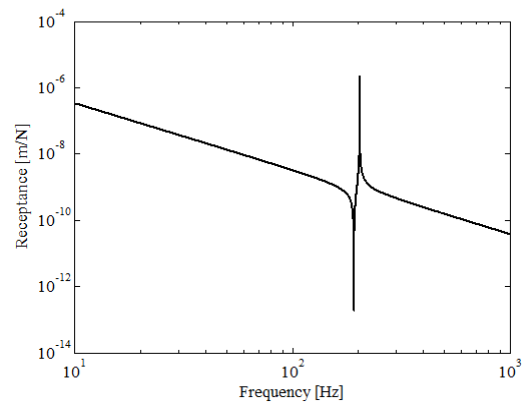


Figure 5. Wheelset receptance for antisymmetric excitation.

The presence of wheelset gear leads to the coupling of symmetrical vibrations with the antisymmetric vibrations due to the asymmetry of the structure (figures 6 and 7). In addition, the resonance frequencies decrease due to inertial effect. These frequencies are at approx. 90 Hz and 191 Hz, respectively. In the case of symmetrical excitation (figure 6), the resonance frequencies are located between the two antiresonance frequencies (85.3 Hz and 193.2 Hz respectively). For antisymmetric wheelset excitation, the resonance frequencies are preceded by an antiresonance frequency at 89 Hz and 187 Hz respectively (figure 7).

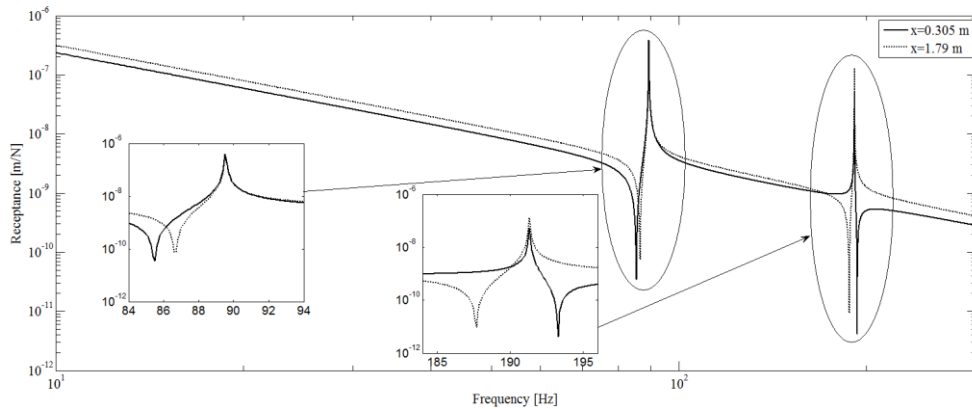


Figure 6. The receptance of the driving wheelset with symmetrical excitation.

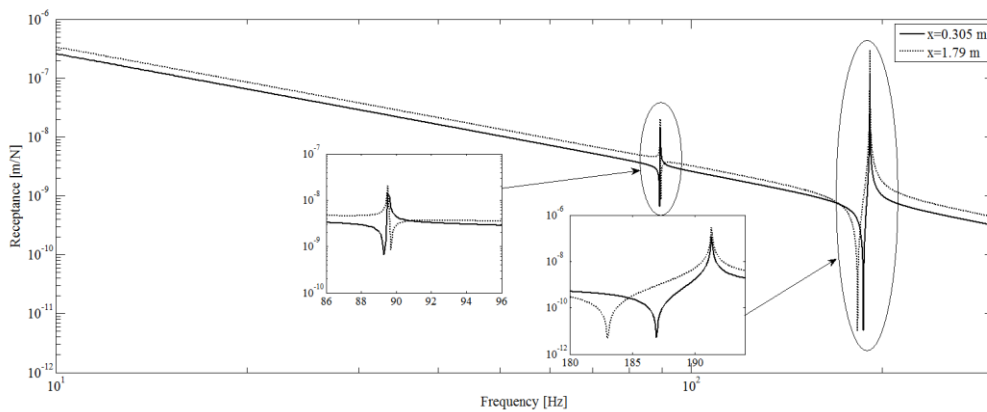


Figure 7. The receptance of the driving wheelset with antisymmetric excitation.

Also, figures 6 and 7 show the receptances calculated against the two wheels when the wheelset is both symmetrically and antisymmetric excited. The lower value of the receptance against the left wheel is explained by the presence of the gear near it. Due to the higher mass on the left side of the wheelset, the inertia increases, and the vertical movement has a lower value.

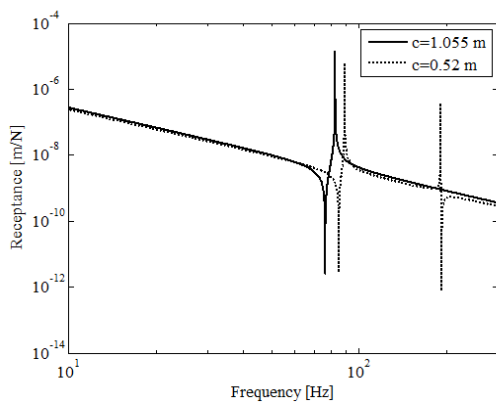


Figure 8. The receptance of the driving wheelset with different position of the gear for symmetrical excitation.

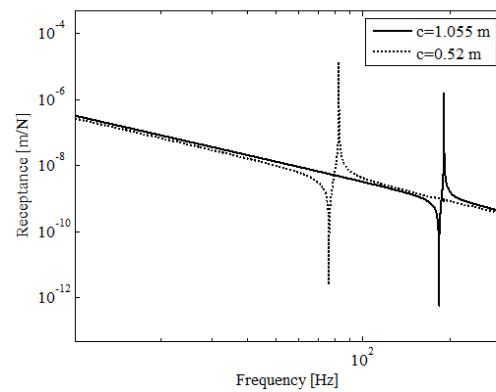


Figure 9. The receptance of the driving wheelset with different position of the gear for antisymmetric excitation.

Figure 8 shows the receptance of the driving wheelset when the gear is placed at the centre of it, compared to the de facto situation. It can be seen that the first resonance and antiresonance frequencies decrease, their value being 83 Hz and 76.6 Hz. Also, due to the decoupling of the two types of vibration, the symmetrical excitation only excites the symmetrically vibration mode. The receptance for the first wheel has a higher value due to the balanced distribution of the inertia force along the wheelset compared to the wheelset whose gear is near the wheel, resulting a greater inertia near the wheel. In the case of antisymmetric excitation (figure 9), only the antisymmetric vibration mode is excited, the resonance frequency being equal to the resonance frequency of the driving wheelset with the gear located near the wheel.

4. Conclusions

In this paper a model with distributed and concentrated parameters has been developed to study the bending vibrations of a driving wheelset for low and medium frequencies. The basic characteristics of bending vibrations have been highlighted by applying the modal analysis method. The model presented will after being embedded in a comprehensive model for studying of driving wheelset-track vibrations.

The first four vibration modes were considered in order to study the influence of wheelset gear on the vibration of the driving wheelset. The presence of the gear results in the reduction of the natural frequencies. Thus, the frequency of the first vibration mode decreases from 95.5 Hz to 90 Hz and the frequency of the second vibration mode decreases from 192.5 Hz to 191 Hz. At the same time, the coupling of the symmetrical modes with the antisymmetric ones takes place, which leads to different receptance on the two wheels, aspect which is likely to favour the occurrence of the torsional vibrations of the driven wheelset.

When the gear is located at the centre of the wheelset, the symmetrical vibration modes are decoupled from the antisymmetric ones.

5. References

- [1] Remington P J 1987 Wheel/rail rolling noise, I: Theoretical analysis *Journal of Acoustical Society of America* **81** 1824-1832
- [2] Thompson D J 1993 Wheel/rail noise generation, part II: wheel vibration *Journal of Sounds and Vibration* **161** 401-419
- [3] Popa G 2005 Tractiunea feroviara cu motoare asincrone trifazate (Bucuresti: MatrixRom)
- [4] Oostermeijer K H 2009 Review on short pitch rail corrugation studies *Wear* **265** 1231-1237
- [5] Mazilu T 2009 On the dynamic effects of wheel running on discretely supported rail *Proceedings of the Romanian Academy, Series A Mathematics, Physics, Technical Sciences, Information Science* **10** 269-276
- [6] Morys B 1999 Enlargement of out of round wheel profiles on high speed trains *Journal of Sounds and Vibration* **227** 965-978
- [7] Mazilu T, Dumitriu M, Tudorache C and Sebesan M 2011 Using the Green's functions method to study wheelset/ballasted track vertical interaction *Mathematical and Computer Modelling* **54** 261-279
- [8] Martínez-Casas J, Giner-Navarro J, Baeza L and Denia F D 2017 Improved railway wheelset-track interaction model in the high-frequency domain *Journal of Computational and Applied Mathematics* **309** 642-653
- [9] Baeza L, Giner-Navarro J, Thompson D J and Monterde J 2019 Eulerian models of the rotating flexible wheelset for highfrequency railway dynamics *Journal of Sounds and Vibration* **449** 300-314